Selective Replacement of Organosilicon Units in the Adamantane-Type Cluster $[(PhSi)_4S_6]$ with Coinage Metal Complex Fragments

Simon Nier[a], Sven Ringelband and Stefanie Dehnen*[a]

[a] S. Nier, Prof. Dr. S. Dehnen
Fachbereich Chemie und Wissenschaftliches Zentrum für Materialwissenschaften (WZMW)
Philipps-Universität Marburg
Hans-Meerwein-Str. 4, 35043 Marburg (Germany)
E-mail: dehnen@chemie.uni-marburg.de

SUPPORTING INFORMATION

1. Experimental Details

General

All manipulations carried out under oxygen- and moisture-free conditions in an argon atmosphere using standard Schlenk or dry-box techniques. THF-d_8 (>99.5%,Sigma-Aldrich) and DMF-d_7 (>99.5%, Sigma-Aldrich) were distilled prior to use and stored under molecular sieves. THF was predried with KOH, dried with potassium and freshly distilled prior to use. *n*-hexane was predried with $CaCl_2$, dried with potassium and freshly distilled prior to use. DMF was dried with P_2O_5 and freshly distilled prior to use. Et_3P (99%, abcr) was used without further purification. Me_3P,[1] $[(PhSi)_4S_6]$,[2] AgCl,[3] and Na_2S[3] were synthezised according to the literature.

X-Ray Crystallography

X-Ray crystal structures were measured with a Mo-Kσ radiation source at 100 K, using a STOE IPDS 2 or a STOE IPDS 2T diffractometer. Reflection data were processed with X-Area 1.[4] The structures were solved by dual space methods in SHELXT[5] and refined by full matrix-least-squares refinement against F^2 in SHELXL[6] using the Olex2[7] user interface.

NMR Spectroscopy

^{1}H, ^{13}C, ^{29}Si, and ^{31}P NMR spectra were recorded on a Bruker AV III HD 250 MHz, AV III HD 300 MHz, AV II 300 MHz or a AV III 500 MHz. The chemical shifts were referenced to solvent signals (THF-d_8: δ(^{1}H) = 3.580 ppm, δ(^{13}C) = 67.570 ppm; DMF-d_7: δ(^{1}H) = 2.920 ppm, δ(^{13}C) = 163.150 ppm;). The raw data were processed with MestReNova 14.2.0-26256.

TGA/DSC Analysis

Thermal properties were investigated using a Netzsch STA 409 CP. Raw data were processed using OriginPro 2017.

Elemental Analysis

µ-XRF data were recorded on a Bruker Tornado M4 equipped with an Rh-target X-Ray tube and a silicon drift detector.

IR Spectroscopy

Infrared spectra were recorded using a Bruker Alpha II or Bruker Tensor 37. Raw data were processed using OriginPro 2017.

UV-Vis Spectroscopy

UV-Vis spectra were recorded on single crystals of compounds **1** and **2** using an Agilent Varian Cary 5000 UV-Vis-NIR spectrophotometer, equipped with a Praying Mantis accessory for solid state samples.

Synthesis of [(Et$_3$PAg)$_3$(PhSi)$_3$S$_6$] (1)

$$[(PhSi)_4S_6]\ (\mathbf{A}) + AgCl + 3\ PEt_3 \xrightarrow[-78\ °C\ \text{to rt in 17 h}]{\text{THF, light exclusion}} [(Et_3PAg)_3(PhSi)_3S_6]\ (\mathbf{1})$$

[(PhSi)$_4$S$_6$] (120 mg, 0.196 mmol, 613.16 g/mol) and AgCl (28 mg, 0.195 mmol, 143.32 g/mol) were dissolved in THF (20 mL) in a flask closed by a septum and wrapped in aluminum foil. Afterwards, the solution was cooled to –78 °C, and Et$_3$P (80 mg, 0.677 mmol, 118.16 g/mol) was added. After addition of the reactants the solution was allowed to slowly warm up to room temperature, and subsequently stirred for 17 h. The colorless reaction solution was layered with *n*-hexane (10 mL). Colorless crystals of **1** formed within 24 h.

Yield: 40 mg (17%, 0.0337 mmol, $C_{36}H_{60}Ag_3P_3S_6Si_3$, 1186.02 g/mol). T_{dec} = 133 °C. **Elemental analysis (µ-XRF):** found (calc.): Si 20.02 (25.00), P 21.70 (25.00), S 58.27 (50.00); all errors are within the error of the method (<1 atom). **IR**: ν = 450, 470, 528, 571, 592, 621, 695, 738, 766, 994, 1042, 1100, 1181, 1249, 1305, 1333, 1376, 1409, 1429.

Synthesis of [Na$_2$(thf)$_{2.33}$][(Me$_3$PCu)(PhSi)$_3$S$_6$]·THF (2·THF)

$$[(PhSi)_4S_6]\ (\mathbf{A}) + CuCl + 3\ PMe_3 + 2\ Na_2S \xrightarrow[-78\ °C\ \text{to rt in 17 h}]{\text{THF, light exclusion}} [Na_2(thf)_{2.33}][(Me_3PCu)(PhSi)_3S_6]\ (\mathbf{2})$$

[(PhSi)$_4$S$_6$] (199 mg, 0.325 mmol, 613.16 g/mol), CuCl (37 mg, 0.374 mmol, 98.99 g/mol.) and Na$_2$S (51 mg, 0.653 mmol, 78.05 g/mol) were dissolved in THF (20 mL) in a flask closed by a septum. Afterwards, the solution was cooled to –78 °C, and Me$_3$P (76 mg, 0.999 mmol, 76.08 g/mol) was added. After addition of the reactants, the solution was allowed to slowly warm up to room temperature, and subsequently stirred for 17 h. The slightly turbid reaction solution was layered with *n*-hexane (10 mL). Colorless crystals of **2** formed within one week.

Yield (vacuum-dried)**:** 22 mg (8%, 0,0438 mmol, $C_{30.33}H_{42.66}Cu_1Na_2O_{2.33}P_1S_6Si_3$ 861.59 g/mol). T_{dec} = <150 °C. **Elemental analysis (µ-XRF):** found (calc.): Cu 13.41 (9.00), Si 21.81 (27.00), P 7.61 (9.00), S 57.17 (54.00); all errors are within the error of the method (<1 atom). **^{29}Si-NMR** (500 MHz, DMF-D$_7$, 300 K): δ = 2.92 ppm. **^{31}P-NMR** (500 MHz, CDCl$_3$, 300 K): δ = -53.63 ppm. **IR**: ν = 453, 477, 539, 613, 633, 707, 750, 967, 1125, 1455.

Alternative Synthetic Access to $[Na_2(thf)_{2.33}][(Me_3PCu)(PhSi)_3S_6]\cdot THF$ (2·THF)

$$[(PhSi)_4S_6]\ (\mathbf{A}) + [CuCl(PMe_3)_3] + 2\ Na_2S \xrightarrow[-78\ °C\ \text{to rt in 17 h}]{\text{THF, light exclusion}} [Na_2(thf)_{2.33}][(Me_3PCu)(PhSi)_3S_6]\ (\mathbf{2})$$

$[(PhSi)_4S_6]$ (92 mg, 0.150 mmol, 613.16 g/mol) and Na_2S (22 mg, 0.281 mmol, 78.05 g/mol) were dissolved in THF (10 mL) in a flask closed by a septum. Afterwards, the solution was cooled to –78°C, and $[CuCl(PMe_3)_3]$ (50 mg, 0.153 mmol, 327.24 g/mol, dissolved in 10 mL of THF), was added over a time span of 15 min. The initially colorless solution turned yellow after 1 h, and brown after another 4 h of stirring at room temperature. A colorless solution is finally obtained after 12 h. The slightly turbid solution was layered with *n*-hexane (10 mL). Colorless crystals of **2** formed within one week. Analyses of the product produce identical results as compared to the analyses of the product obtained by the other method.

2. Crystallographic Details

Table S1. Crystallographic details of $[(Et_3PAg)_3(PhSi)_3S_6]$ (1) and $[Na_2(thf)_{2.33}][(Me_3PCu)(PhSi)_3S_6]\cdot THF$ (2·THF).

compound	**1**	**2·THF**
Sum Formula	$C_{36}H_{60}Ag_3P_3S_6Si_3$	$C_{30.22}H_{42.66}CuNa_2O_{2.33}PS_6Si_3\cdot C_4H_8O$
Empirical formula	$C_{36}H_{60}Ag_3P_3S_6Si_3$	$C_{91}H_{128}Cu_3Na_6O_7P_3S_{18}Si_9\cdot 3C_4H_8O$
Formula weight [g/mol]	1185.99	2801.60
Crystal color, shape	colorless, clear, block	Colorless, block
Crystal system	orthorhombic	triclinic
Space group	$Pna2_1$	$P\bar{1}$
a [Å]	40.1788(14)	19:0521(9)
b [Å]	21.4061(7)	19.7933(3)
c [Å]	11.3403(3)	21.5839(9)
α [°]	90	107.582(3)
β [°]	90	115.295(3)
γ [°]	90	99.475(3)
V [Å^3]	9753.5(5)	6595.4(5)
Z	8	2
ρ_{calc} [g/cm^3]	1.615	1.411
μ (Mo K_α) [mm^{-1}]	1.647	0.953
Absorption correction type	numerical	numerical
Min. / max. transmission	0.8242/ 0.9141	0.8481/0.8490
2ϑ range [°]	2.156-51.340	1.91-54.78
Reflections measured	75912	86552
R(int)	0.0443	0.0524
Parameters	938	1333
Restraints	1	0
$R1$ ($I > 2\sigma(I)$)	0.0265	0.0406
$R1$ (all data)	0.0384	0.0582
wR2	0.0536	0.1055
GooF (all data)	0.907	1.037
Max. peak/ hole [e$^-$/ Å^3]	0.981/ –0.603	1.830/ –0.810
Flack parameter	0.496(17)	–
CCDC number	2100213	2100214

Table S2. Selected bond lenghts [Å] and angles [°] of compound 1.

Ag1–S3	2.5960(17)	P1–Ag1–S2	113.43(5)	Si2–S4–Si1	106.01(9)
Ag1–S1	2.7028(17)	P1–Ag1–S1	122.89(6)	Si3–S5–Si1	105.39(9)
Ag1–P1	2.4268(17)	S3–Ag1–S1	94.38(5)	Si3–S6–Si2	112.20(9)
Ag1–S2	2.6015(16)	P2–Ag2–S2	151.91(6)	S4–Si1–S5	109.51(10)
Ag2–S1	2.7580(16)	P2–Ag2–S1	105.87(5)	S1–Si1–S5	115.16(10)
Ag2–S2	2.4634(16)	S2–Ag2–S1	98.48(5)	C7–Si1–S1	110.6(2)
Ag2–P2	2.3688(17)	P3–Ag3–S3	158.73(6)	C7–Si1–S4	103.6(2)
Ag3–P3	2.3791(19)	P3–Ag3–S1	105.18(6)	C7–Si1–S5	103.7(2)
Ag3–S3	2.4977(17)	S3–Ag3–S1	94.90(5)	S1–Si1–S4	113.29(10)
Ag3–S1	2.7741(16)	Ag1–S1–Ag3	76.06(4)	S2–Si2–S6	113.81(10)
S1–Si1	2.071(2)	Ag2–S1–Ag3	145.78(7)	S6–Si2–S4	111.09(10)
S2–Si2	2.083(2)	Si1–S1–Ag1	107.59(8)	C1–Si2–S2	110.7(2)
S3–Si3	2.082(2)	Si1–S1–Ag2	97.39(8)	C1–Si2–S4	102.9(2)
S4–Si2	2.152(2)	Ag1–S1–Ag2	69.84(4)	S2–Si2–S4	115.29(10)
S4–Si1	2.152(2)	Si1–S1–Ag3	89.95(7)	C1–Si2–S6	101.7(2)
S5–Si1	2.160(2)	Si2–S2–Ag2	97.87(8)	C13–Si3–S6	102.4(2)
S5–Si3	2.156(2)	Si2–S2–Ag1	100.22(8)	C13–Si3–S5	103.5(2)
S6–Si3	2.138(2)	Ag2–S2–Ag1	76.18(5)	C13–Si3–S3	110.1(2)
S6–Si2	2.146(2)	Si3–S3–Ag1	100.85(8)	S3–Si3–S5	113.19(10)
S3–Ag1–S2	121.08(5)	Ag3–S3–Ag1	82.96(5)	S6–Si3–S5	110.58(10)
S2–Ag1–S1	96.56(5)	Si3–S3–Ag3	93.72(7)	S3–Si3–S6	115.76(10)
P1–Ag1–S3	107.85(6)				

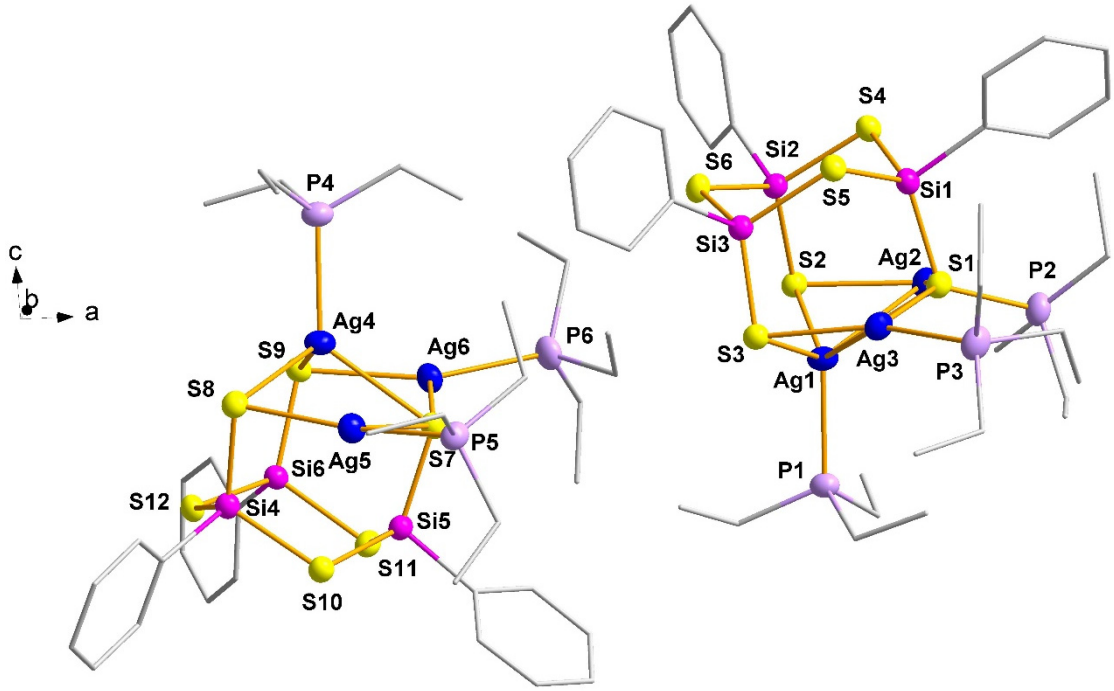

Figure S1. Diamond representation of the asymmetric unit of compound 1, comprising two individual and crystallographically independent cluster molecules. Thermal ellipsoids shown at 50% probability level. Hydrogen atoms are omitted and carbon atoms are illustrated as wires/sticks model for clarity.

Table S3. **Selected bond lenghts [Å] and angles [°] of compound 2.**

S9–Na2	2.9010(13)	Cu1–S1	2.3639(8)	S3–Na2–S5	67.46(3)
S8–Na2	2.9607(14)	Cu1–P1	2.2355(8)	S8–Na2–S12	67.56(3)
S8–Si5	2.0782(10)	Cu1–S2	2.3621(8)	S8–Na2–S5	169.62(5)
S6–Na6	3.1769(13)	S2–Cu1–S1	111.12(3)	S8–Na2–S3	110.55(4)
S6–Si2	2.1477(10)	S1–Cu1–S3	110.36(3)	S1–Na2–S5	69.56(3)
S6–Si3	2.1486(10)	S2–Cu1–S3	111.99(3)	S1–Na2–S9	135.74(5)
S5–Na2	3.3367(14)	P1–Cu1–S3	111.86(3)	S1–Na2–S12	86.73(4)
S5–Si3	2.1568(10)	P1–Cu1–S1	108.22(3)	S9–Na2–S8	83.14(3)
S5–Si1	2.157(1)	P1–Cu1–S2	103.05(3)	S9–Na2–S3	125.63(5)
S4–Si1	2.1781(10)	Si1–S1–Cu1	100.25(4)	S9–Na2–S5	89.96(4)
S4–Na1	2.9964(14)	Cu1–S1–Na2	79.10(3)	S9–Na2–S12	67.65(3)
S4–Si2	2.1525(10)	Cu1–S1–Na1	83.38(3)	S1–Na2–S8	120.71(4)
S3–Na2	3.0012(14)	Si1–S1–Na2	93.61(4)	Si3–S3–Cu1	100.34(4)
S3–Si3	2.0744(10)	Si6–S12–Na2	80.75(3)	Si3–S3–Na6	88.83(4)
S3–Na6	2.9602(14)	Si5–S12–Na2	81.46(3)	Na6–S3–Na2	153.92(4)
S2–Si2	2.0587(10)	Si2–S2–Na6	90.23(4)	Si2–S4–Si1	105.59(4)
S2–Na6	2.9532(14)	Na6–S2–Na1	156.52(4)	Si1–S4–Na1	83.34(4)
S2–Na1	3.1203(14)	Cu1–S2–Na6	78.31(3)	Si2–S4–Na1	86.00(4)
S12–Na2	3.4102(14)	Cu1–S2–Na1	80.29(3)	Si3–S5–Na2	83.87(4)
S6–Na6–S17	106.21(4)	Si2–S2–Na1	84.37(4)	Si3–S5–Si1	105.44(4)
S2–Na6–S6	70.23(3)	Si2–S2–Cu1	100.77(3)	Si1–S5–Na2	79.46(4)
S2–Na6–S3	83.26(3)	Si3–S3–Na2	94.33(4)	Si3–S6–Na6	82.02(4)
S2–Na6–S17	97.94(4)	Cu1–S3–Na2	76.01(3)	Si2–S6–Na6	82.86(4)
S2–Na6–S15	125.93(4)	Cu1–S3–Na6	77.95(3)	Si2–S6–Si3	108.15(4)
S15–Na6–S6	163.16(5)	O3–Na1–S2	122.86(8)	C1–Si1–S5	102.44(9)
S13–Na6–S2	143.91(5)	O1–Na1–S4	85.36(6)	S1–Si1–S4	114.12(4)
S13–Na6–S6	80.75(3)	O1–Na1–S1	107.51(7)	S5–Si1–S4	110.39(4)
S3–Na6–S17	176.41(5)	O1–Na1–S2	152.65(7)	S1–Si1–S5	115.02(4)
S3–Na6–S15	112.74(4)	O2–Na1–O1	86.33(8)	C1–Si1–S1	112.07(10)
S3–Na6–S6	70.95(3)	O2–Na1–S4	107.27(7)	C1–Si1–S4	101.34(9)
S13–Na6–S3	107.52(4)	O3–Na1–S4	150.42(8)	S2–Si2–S6	114.15(4)
Si1–S1–Na1	85.82(4)	S1–Na1–S2	79.43(3)	C13–Si2–S6	101.56(9)
Na2–S1–Na1	162.09(4)	S1–Na1–S4	73.07(3)	C13–Si2–S2	111.64(9)
S1–Na2	2.8591(14)	S4–Na1–S2	71.16(3)	C13–Si2–S4	104.93(9)
S1–Na1	2.9773(14)	O2–Na1–S2	87.46(7)	S2–Si2–S4	115.42(5)
S1–Si1	2.0586(10)	O2–Na1–S1	166.05(8)	S6–Si2–S4	107.88(4)
P1–C33	1.806(4)	O3–Na1–S1	83.69(7)	C7–Si3–S5	103.57(9)
P1–C32	1.815(3)	O3–Na1–O1	84.45(9)	C7–Si3–S3	113.13(9)
P1–C31	1.813(4)	O3–Na1–O2	99.70(9)	C7–Si3–S6	101.48(10)
Na1–O3	2.325(3)	S1–Na2–S3	83.18(3)	S3–Si3–S5	113.09(5)
Na1–O2	2.337(2)	S5–Na2–S12	116.85(4)	S3–Si3–S6	115.21(4)
Na1–O1	2.392(2)	S3–Na2–S12	166.69(4)	S6–Si3–S5	109.16(4)
Cu1–S3	2.3766(8)				

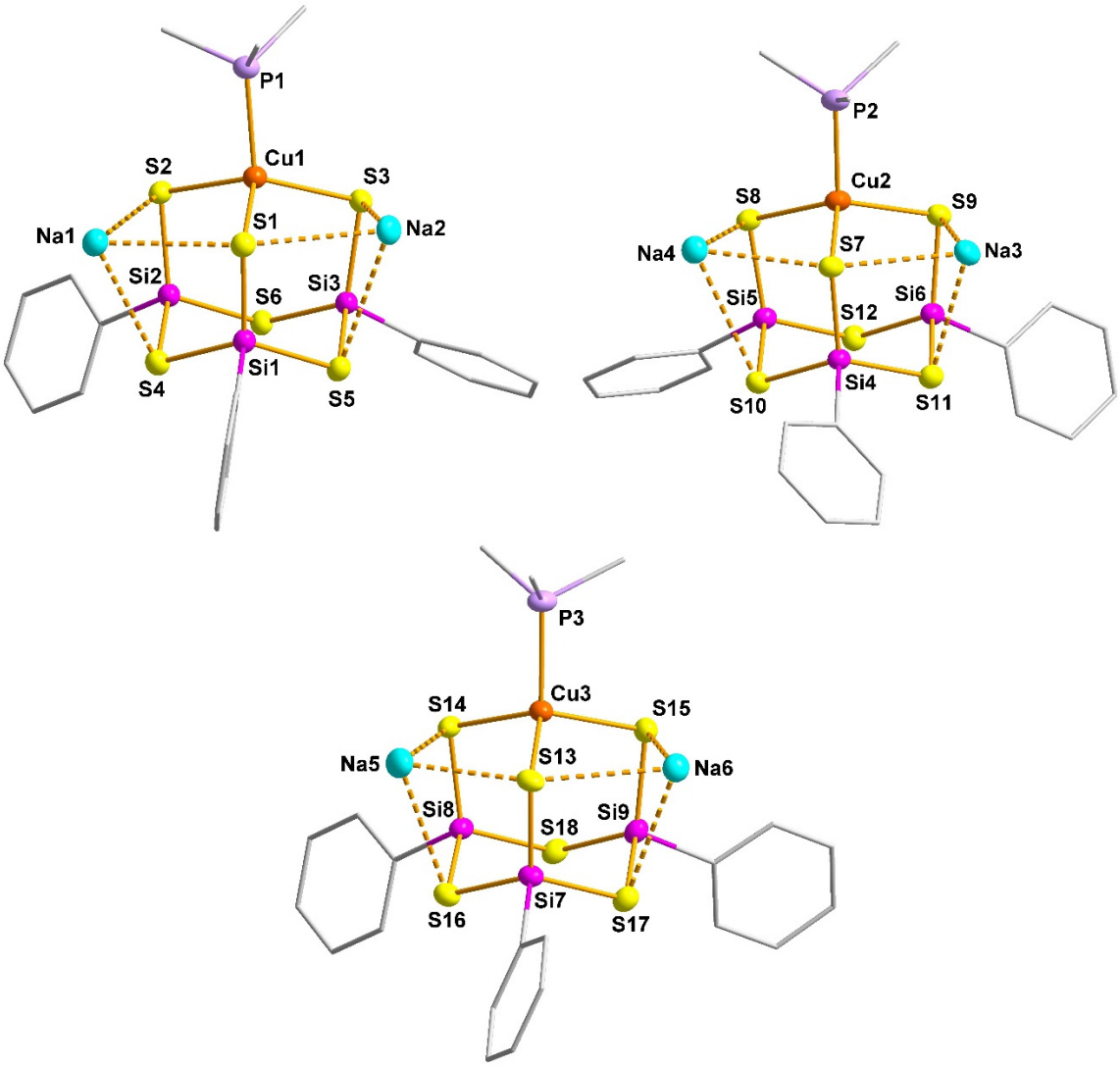

Figure S2. Diamond representation of the three individual and crystallographically independent cluster molecules in compound 2. Thermal displacement ellipsoids shown at 50% probability level. Hydrogen atoms and THF molecules at Na1, Na3, and Na5 are omitted and carbon atoms are illustrated as wires/sticks model for clarity.

3. NMR Spectroscopy

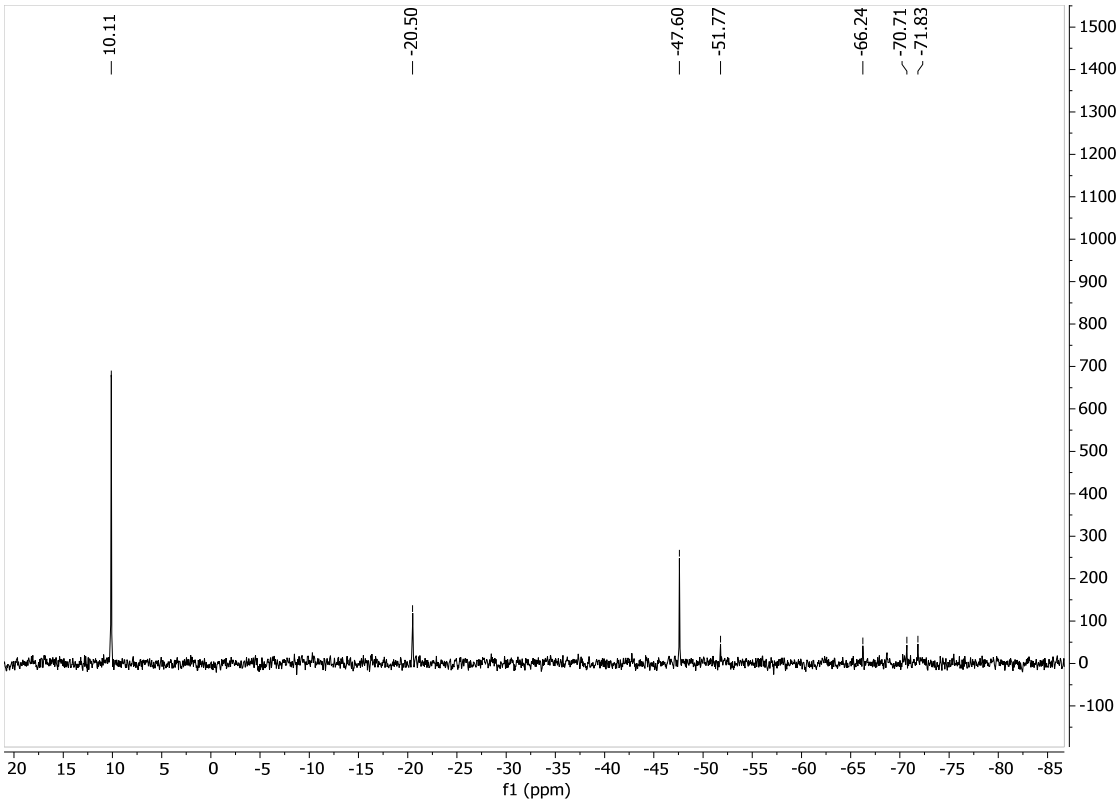

Figure S3. ^{29}Si NMR spectrum from reaction solution before crystallization of compound 1 in THF-d$_8$.

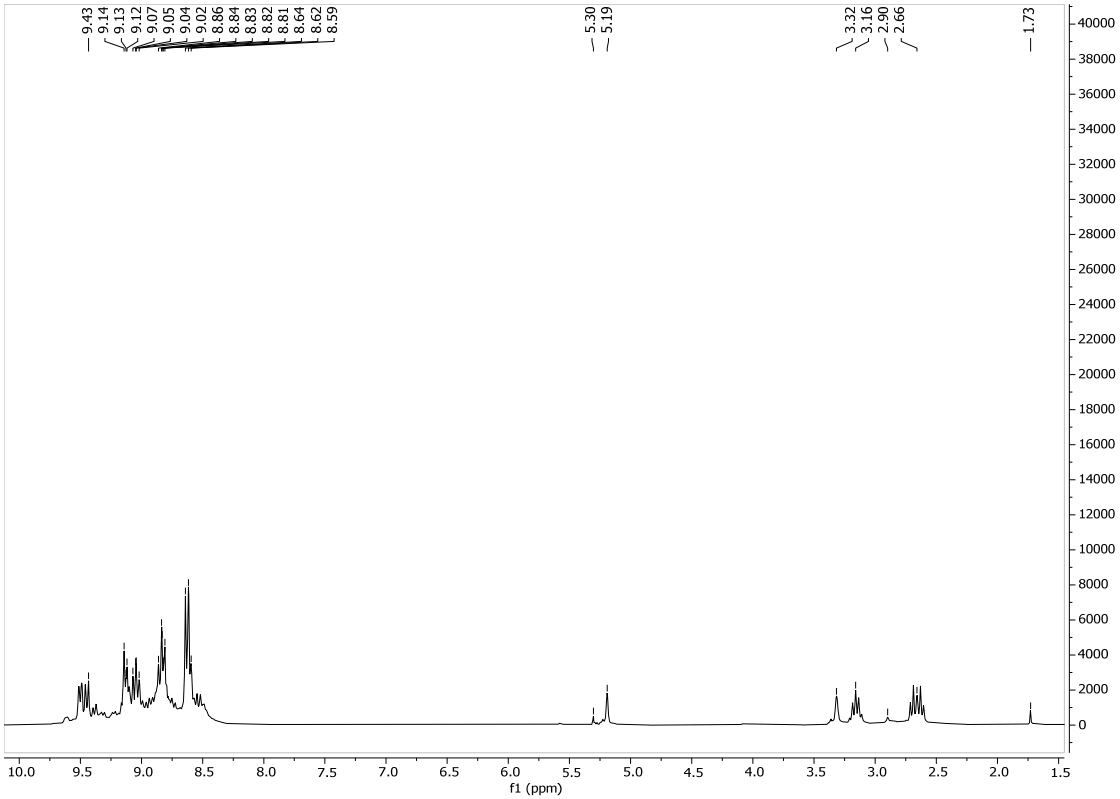

Figure S4. ^{1}H NMR spectrum from reaction solution before crystallization of compound 1 in THF-d$_8$.

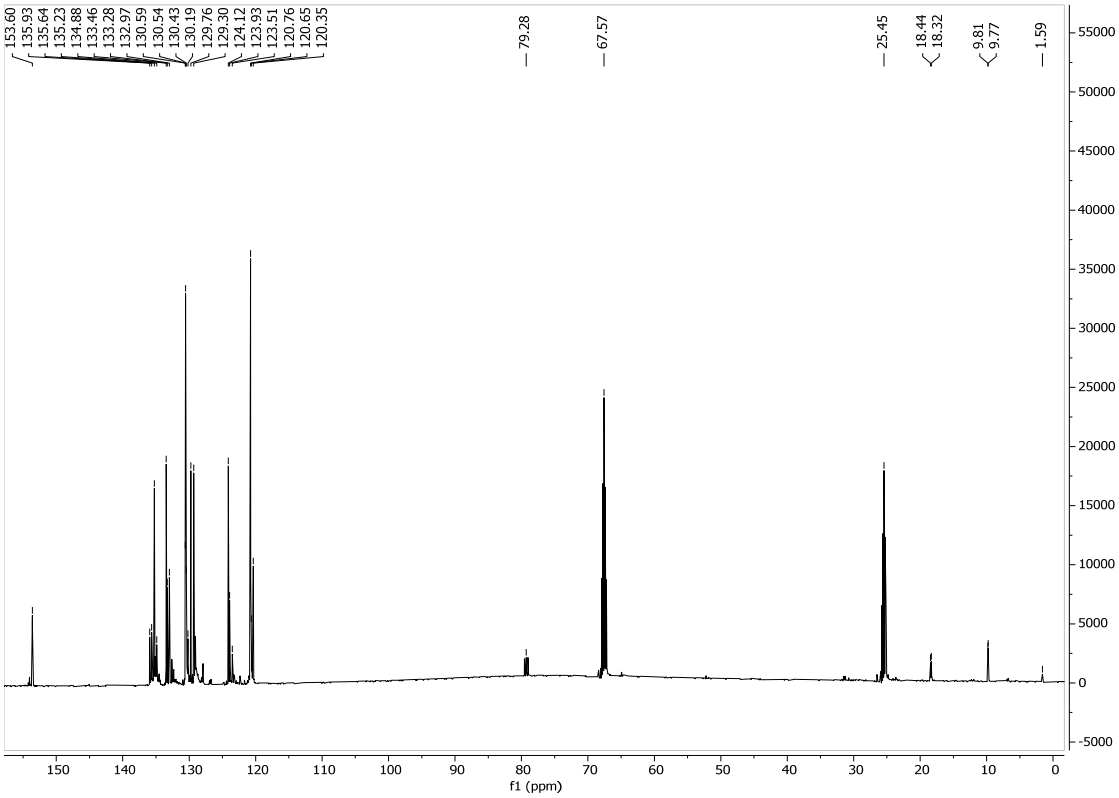

Figure S5. ^{13}C NMR spectrum from reaction solution before crystallization of compound 1 in THF-d_8.

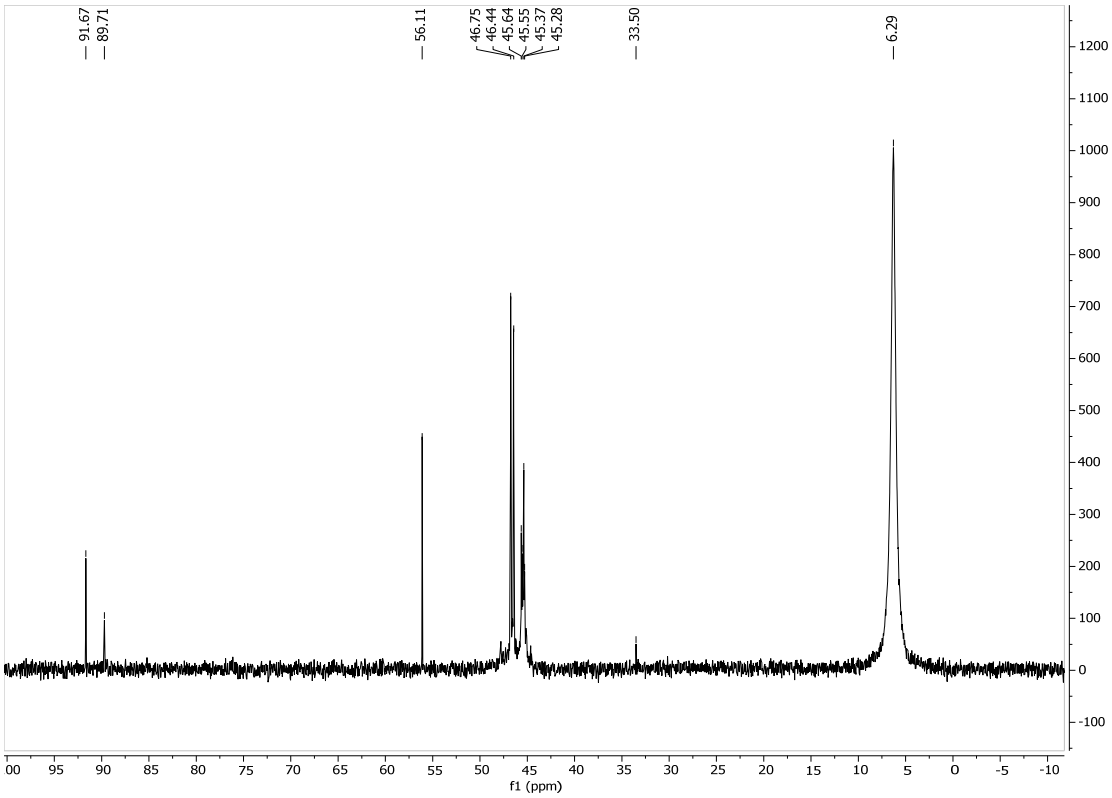

Figure S6. ^{31}P NMR spectrum from reaction solution before crystallization of compound 1 in THF-d_8.

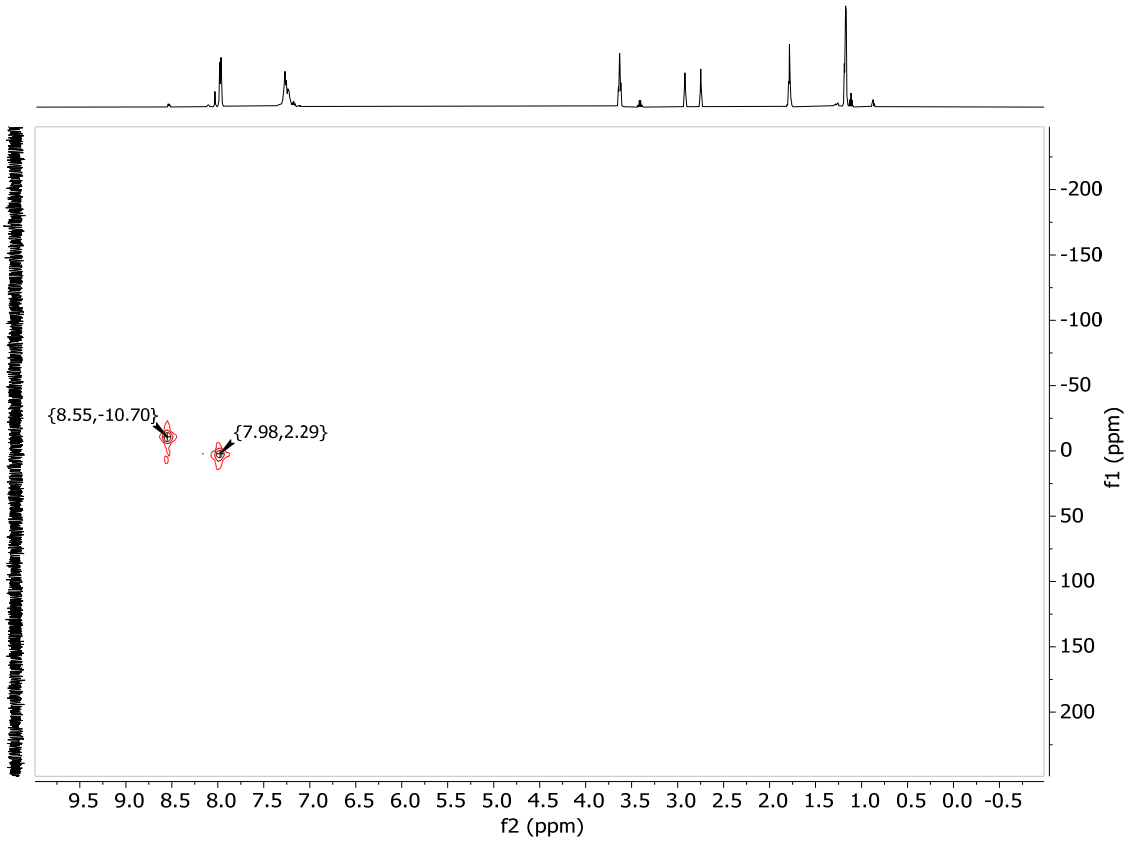

Figure S7. $^{1}H^{29}Si$-HMBC spectrum of compound 2 in DMF-d_7.

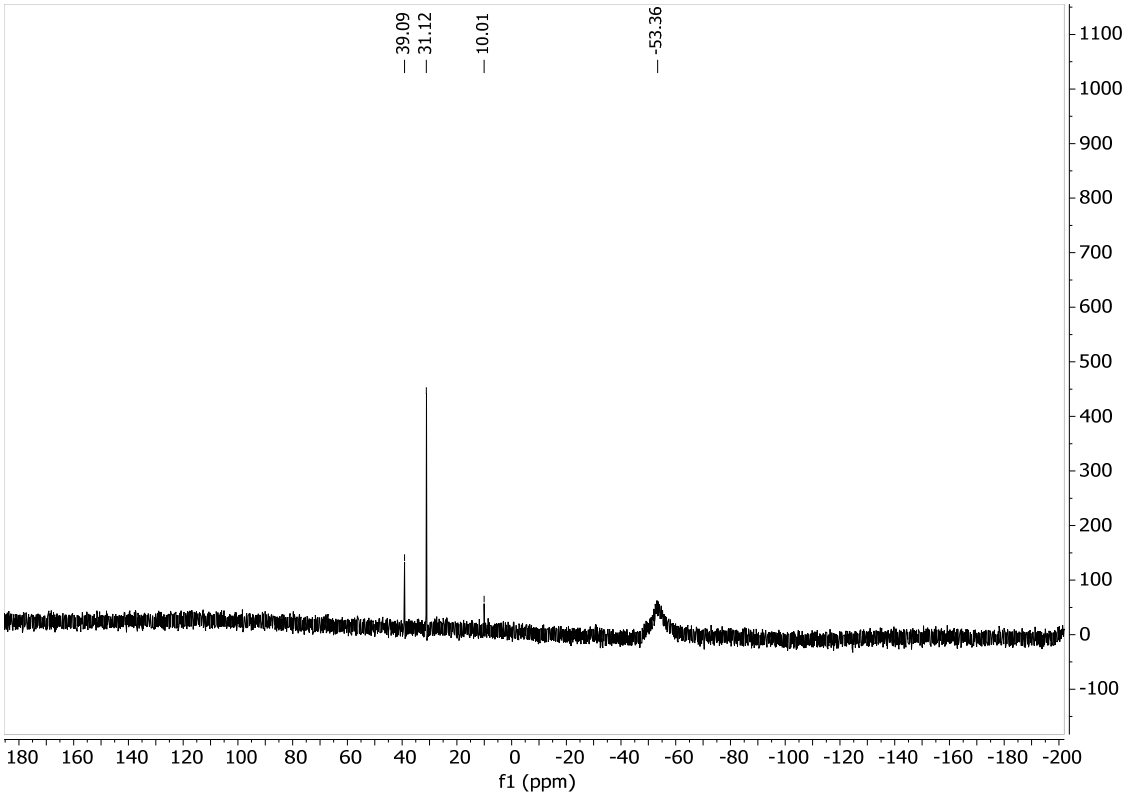

Figure S8. ^{31}P NMR spectrum of compound 2 in DMF-d_7.

4. Thermal Properties

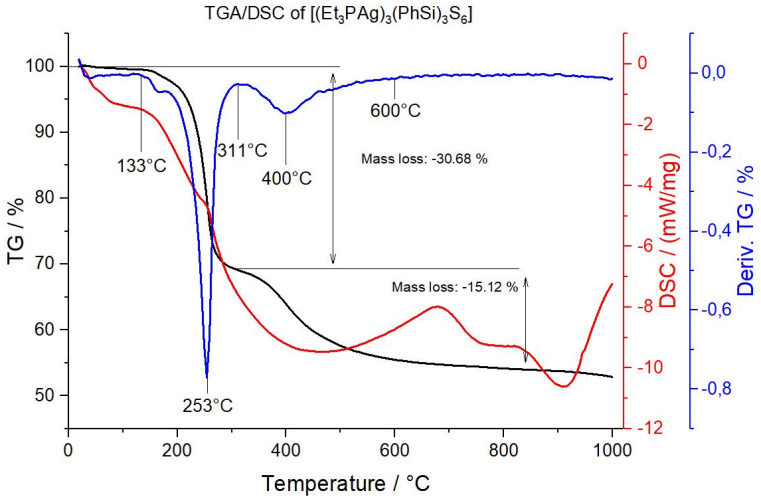

Figure S9. TGA/DSC results for compound 1 (black: TGA, red: DSC, blue: first derivative of TGA).

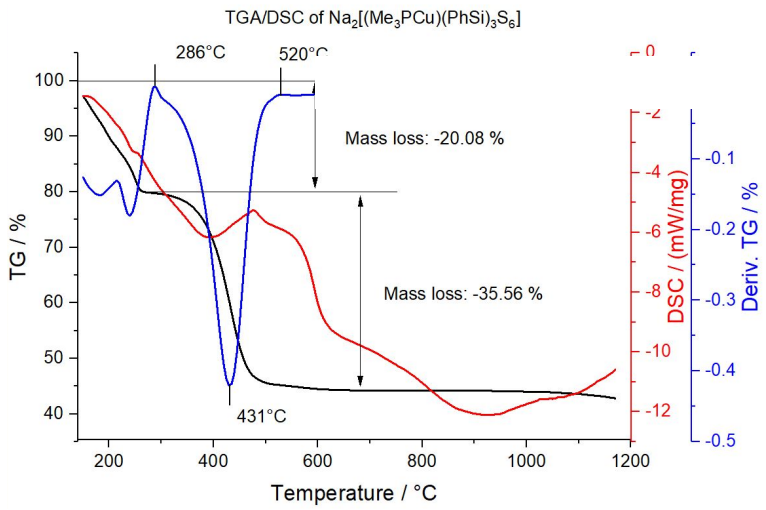

Figure S10. TGA/DSC results for compound 2 (black: TGA, red: DSC, blue: first derivative of TGA). The sample was dried in vacuum prior to the measurement.

The TGA measurements indicate that the cluster core of **1** remains stable up to ~130°C, before a drop in weight down to ~70% sets in with maximum slope at 253 °C, and after a small quasi-plateau, the cluster decomposes entirely above ~400 °C, ending up at a residual mass of ~55%. For **2**, the situation is slightly different, as a loss of {$CuPMe_3$} fragment (20.08% of the weight) causes a continuous weight drop that starts below 150°C and continues until ~280 °C, where the sample mass reaches ~80%. Here, a quasi-plateau is also established up to ~400 °C, above which the compound fully decomposes to a residual mass of ~45% with a maximum slope at 431 °C. The mass losses are in accordance with the different chemical natures and compositions of **1** and **2**. The residue comprises a ternary solid in the first and a quaternary solid in the second case, as expected.

5. Elemental Analysis

Table S4. µ-XRF data of compound 1. Note that the Ag content could not be reliably determined owing to the very similar electron density of the element Ag and the element Rh used as X-ray source.

Element	X-Ray Series	Norm. Cont. (wt%)	Atom Cont. (at.%)	Atom C. calc. (at.%)	Error (1σ [wt.%])
Si	K series	18.12	20.02	25.00	0.01
P	K series	21.66	21.70	25.00	0.01
S	K series	60.21	58.27	50.00	0.01

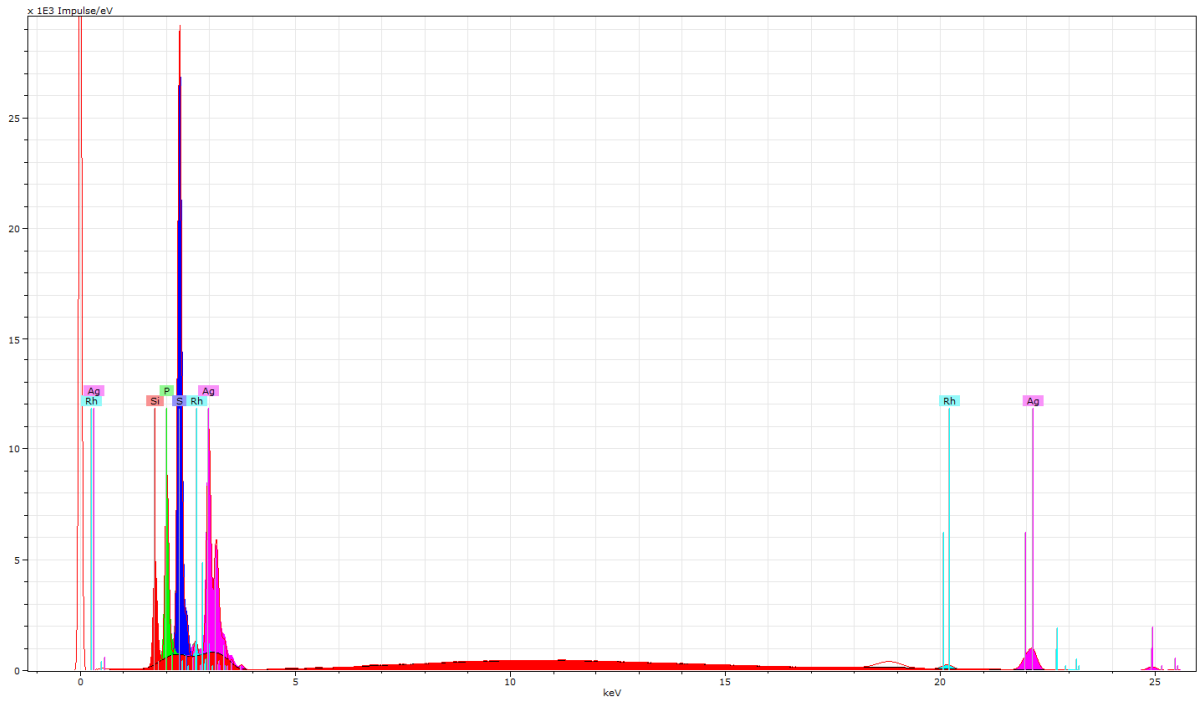

Figure S11. µ-XRF spectrum of compound 1 with polynomial integral fit (Ag: pink; Si: red; P: green; S: blue). Slight deviations are within the error of the method (<1 atom).

Table S5. µ-XRF data of compound 2. Note that a quantitative analysis of Na and all lighter elements is generally not possible with the µ-XRF device.

Element	X-Ray Series	Norm. Cont. (wt%)	Atom Cont. (at.%)	Atom C. calc. (at.%)	Error (1σ [wt.%])
Cu	K series	24.11	13.41	9.00	0.01
Si	K series	17.34	21.81	27.00	0.02
P	K series	6.67	7.61	9.00	0.00
S	K series	51.88	57.17	54.00	0.13

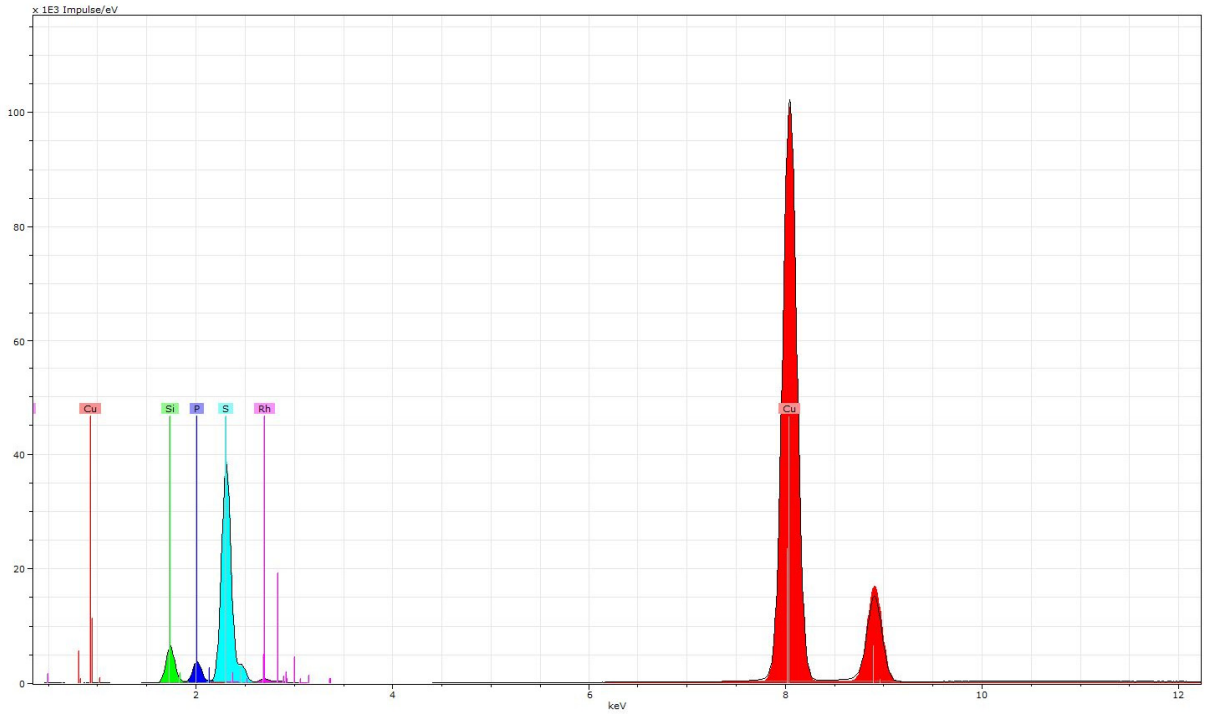

Figure S12. µ-XRF spectrum of compound 2 with polynomial integral fit (Cu: red; Si: green; P: blue; S: turquoise). Slight deviations are within the error of the method (<1 atom).

6. Infrared Spectroscopy

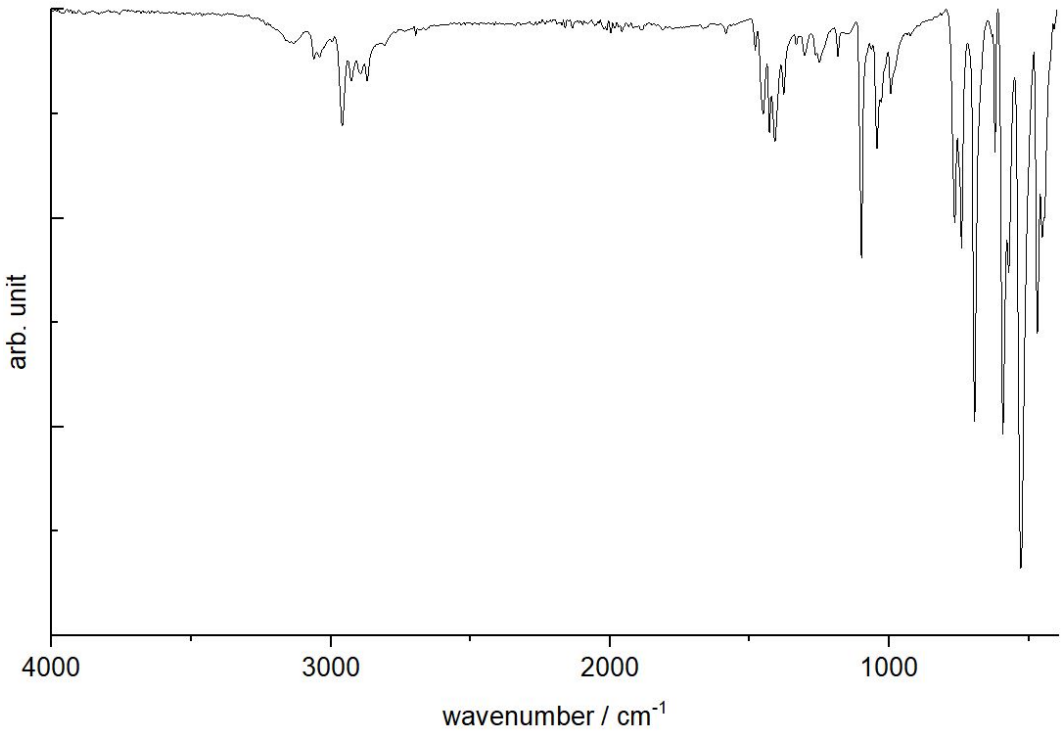

Figure S13.Infrared spectrum of compound 1.

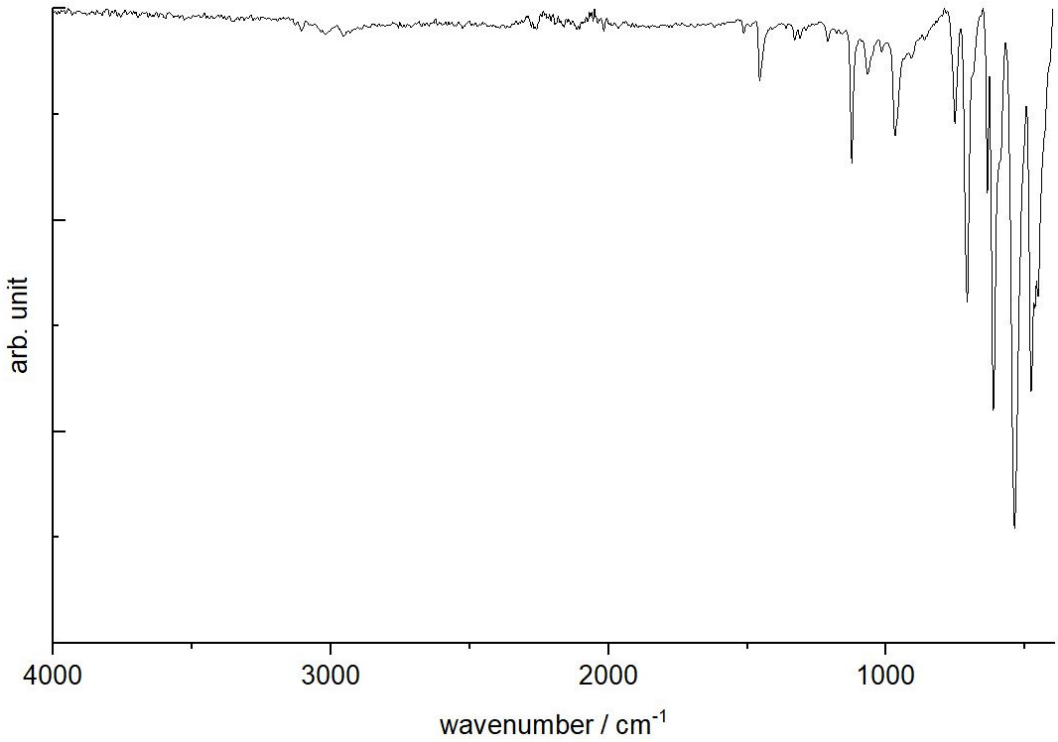

Figure S14. Infrared spectrum of compound 2.

7. UV-Visible Spectroscopy

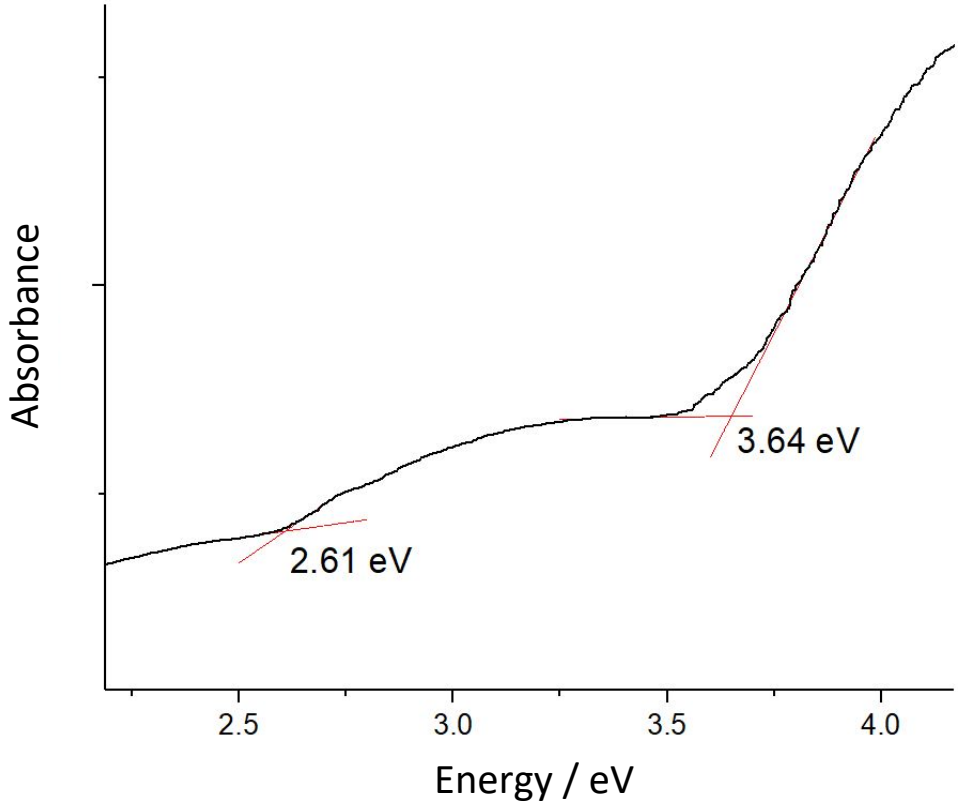

Figure S15 UV-visible spectrum of compound 1 in the solid state.

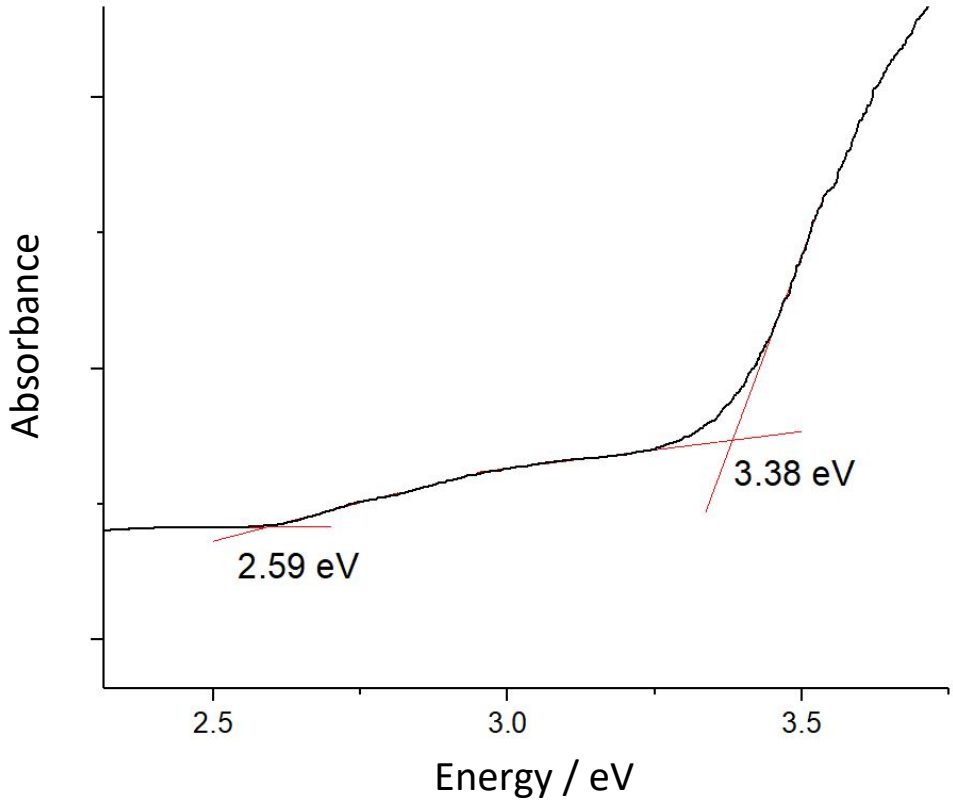

Figure S16.UV-visible spectrum of compound 2 in the solid state.

8. References for the Supporting Information

1 M. L. Luetkens, A. P. Sattelberger, H. H. Murray, J. D. Basil, J. P. Fackler, R. A. Jones, D. E. Heaton (Eds.) *Inorganic Synth*, John Wiley & Sons, New York, Chichester, Brisbane, Toronto, Singapore, **2007**.

2 N. W. Rosemann, J. P. Eußner, E. Dornsiepen, S. Chatterjee, S. Dehnen, *J. Am. Chem. Soc.* **2016**, *138*, 16224.

3 G. Brauer (Ed.) *Handbuch der Präparativen Anorganischen Chemie*, Ferdinand Enke Verlag, Stuttgart, **1975**.

4 Stoe and Cie GmbH, X-Area, Version 1.77, **2016**.

5 G. M. Sheldrick, *Acta Crystallogr.*, *Sect. A* **2015**, *71*, 3-8.

6 G. M. Sheldrick, *Acta Crystallogr.*, *Sect. C* **2015**, *71*, 3-8.

7 O. V. Dolomanov, L. J. Bourhis, R. J. Gildea, J. A. K. Howard, H. Puschmann, *J. Appl. Crystallogr.* **2009**, *42*, 339-341.